Generating Spectra from Ground-State Wave Functions: Unraveling Anharmonic Effects in the $OH^- \cdot H_2O$ Vibrational Predissociation Spectrum†

Anne B. McCoy*

Department of Chemistry, The Ohio State University, Columbus, Ohio 43210

Eric G. Diken and Mark A. Johnson

Department of Chemistry, Yale University, New Haven, Connecticut 06520

Received: December 23, 2008; Revised Manuscript Received: February 07, 2009

An approach is described for calculating anharmonic spectra for polyatomic molecules using only the ground-state probability amplitude. The underlying theory is based on properties of harmonic oscillator wave functions and is tested for Morse oscillators with a range of anharmonicities. More extensive tests are performed with $H_3O_2^-$, using the potential and dipole surfaces of Bowman and co-workers [*J. Am. Chem. Soc.* **2004**, *126*, 5042]. The resulting energies are compared to earlier studies that employed the same potential surface, and the agreement is shown to be very good. The vibrational spectra are calculated for both $H_3O_2^-$ and $D_3O_2^-$. In the case of $H_3O_2^-$, comparisons are made with a previously reported experimental spectrum below 2000 cm^{-1}. We also report the spectrum of $H_3O_2^-$ from 2400−4500 cm^{-1}, which extends 500 cm^{-1} above the region reported earlier, revealing several new bands. As the only fundamentals in this spectral region involve the OH stretches, the spectrum is surprisingly rich. On the basis of comparisons of the experimental and calculated spectra, assignments are proposed for several of the features in this spectral region.

Introduction

With recent technological advances, spectra of molecular ions over frequency ranges from as low as 600 to above 4500 cm^{-1} have been reported for a variety of molecular ions.[1−8] In these experiments, action spectroscopies are employed to detect the relatively small number of ions that are vibrationally excited. Specifically, a chemical reaction or dissociation of weakly attached rare gas atoms is used to identify at what frequencies the molecule absorbs a photon. Using these approaches, a variety of transient and highly fluxional species have been studied in the gas phase.

At the same time, computers and electronic structure programs have developed to the point that it is reasonably straightforward to calculate the spectrum of a molecule of interest at the harmonic level, fully ab initio. Such treatments often work well for fundamentals in the high frequency stretching and bending modes. The harmonic approach breaks down in other regions of the spectrum due to large anharmonicities or to contributions to the spectrum from combination bands. Such problems are encountered in a variety of molecules,[3,9−12] and we will use the complex of OH^- with H_2O as an illustration. This complex is bound by 25 kcal mol^{-1}.[13] Based on the potential surface, it is best thought of as two OH^- molecules separated by a shared proton that is located near the center of the OO bond, in the minimum energy structure. The experimental and harmonic spectra of $H_3O_2^-$ below 2000 cm^{-1} are shown in Figure 1. As is seen in this plot, it is hard to identify many similarities between the experimental and harmonic spectra in this frequency range. In the OH stretch region, near 3500 cm^{-1} the calculated spectrum contains two peaks that correspond to a symmetric and asymmetric stretch and, once appropriate scaling is accounted for, are in reasonable agreement with the position of the OH stretch band in the experimental spectrum.[14]

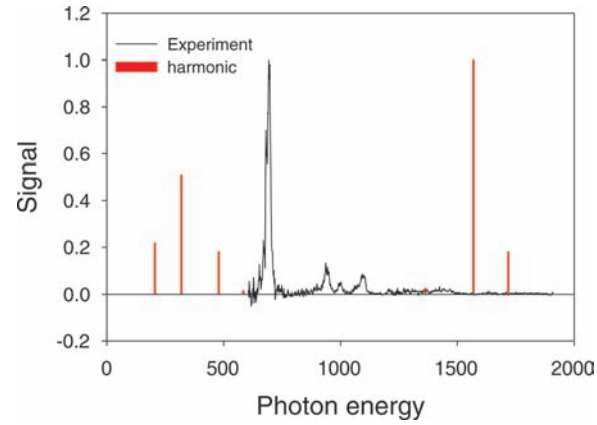

Figure 1. A comparison of the experimental (black)[1] and harmonic (red) spectra of $H_3O_2^-$ below 2000 cm^{-1}. The harmonic spectra were calculated using the potential and dipole surfaces from ref 14.

Clearly the harmonic approximation fails for $H_3O_2^-$. The failures come both from large anharmonicities and from combination bands that carry significant oscillator strength. Such corrections can be introduced using second-order perturbation theory (VPT2) or vibrational self-consistent field (VSCF) approaches,[15−17] both of which have been implemented in electron structure programs.[18,19] For very anharmonic systems, however, these approaches can fail.[20] In the case of $H_3O_2^-$, the barrier for exchange of the central hydrogen atom between the two OH groups is only 0.3 kcal mol^{-1}.[13] This leads us to anticipate that VPT2 and VSCF treatments based on expansions of the potential about its minimum will fail to reproduce the low frequency region of the spectrum.

† Part of the "Robert Benny Gerber Festschrift".

* Corresponding author. E-mail: mccoy@chemistry.ohio-state.edu.

10.1021/jp811352c CCC: $40.75
Published on Web 03/24/2009

A powerful approach for obtaining fully anharmonic ground-state wave functions and zero-point energies is Diffusion Monte Carlo (DMC).[21−23] When potential surfaces are available, DMC has proven to be a highly effective and accurate approach for studying anharmonic molecules. While much of the earlier work with this approach focused on hydrogen-bonded clusters,[22,24−27] more recent studies have included more strongly bound species, including $H_5O_2^+$,[20,28] CH_5^+,[29,30] and $H_3O_2^-$.[1,31]

Because DMC simulations employ statistical approaches to generate the long-time solution to the imaginary time, time-dependent Schrödinger equation, DMC is rigorously a ground-state method. Excited states provide challenges. A variety of approaches have been proposed for evaluating excited-state energies and wave functions. One choice involves taking the inverse Lorentz transform of the appropriate correlation function, obtained from a Quantum Monte Carlo simulation.[32] This is the basis of the POITSE method used by Whaley and co-workers.[33] An alternative approach that we have had good success with is fixed-node DMC.[34] The drawback of this method comes from the fact that each excited state needs to be considered independently. In addition, while this approach is effective for generating the excited state with the property that the wave function changes sign at a specified value of the internal coordinates, care must be taken to ensure that the desired state is probed.[31,35] We have applied this method to a number of systems, including calculations of the nine fundamental frequencies in $H_3O_2^-$, where we could compare to vibrational−configuration interaction calculations, performed using the same potential surface.[31] A third approach was proposed by Coker and Watts[36,37] and applied to studies of the anharmonic spectra of water clusters. In this treatment, they fit the ground-state wave function, obtained from DMC, to ground-state wave functions for a set of uncoupled Morse oscillators. They then extract from the wave functions the corresponding potentials and use them to develop a basis for a variational calculation.

In this Article, we present a slightly different approach for generating spectra based on the ground-state DMC wave function. This approach differs from those described above in that the goal of this study is to develop the expressions that are needed to reexpress all of the quantities needed to generate a spectrum as expectation values involving the ground-state probability amplitude. In addition, because the wave function is not in a form that is easily differentiated, only multiplicative operators will be used. If successful, most of the computer time required for these simulations will be used in evaluating the ground-state probability amplitudes, which we generate using the descendent weighting approach.[22] While the proposed approach is similar in spirit to that of Coker and Watts[36,37] in that we generate our description of excited states from only ground-state information, instead of using the ground-state wave function to generate a basis set for further calculations, we derive all necessary energy and intensity expressions in terms of the ground-state probability amplitude.

To test this approach, we calculate the spectral features in $H_3O_2^-$ and $D_3O_2^-$ that arise from fundamental transitions as well as overtone transitions and combination bands that involve excitation of at most two quanta. The transition frequencies for the fundamentals are compared to previously calculated anharmonic frequencies using the same potential surface.[31] We also compare the calculated spectrum for $H_3O_2^-$ to the spectrum that has been obtained by vibrational predissociation of $Ar\cdot H_3O_2^-$ for energies between 600 and 1900 cm^{-1}.[1] Finally, we report the spectrum of $Ar\cdot H_3O_2^-$ between 2400 and 4500 cm^{-1} and compare the experimental and calculated spectra in this region.

2. Experimental Details

Vibrational predissociation spectra of the size-selected ions were obtained using the Yale tandem time-of-flight, double focusing photofragmentation spectrometer described previously.[38] Argon-solvated cluster anions were prepared in a pulsed supersonic expansion (10 Hz) in which slow secondary electrons were introduced by ionization with a counter-propagating electron beam (1 keV). The $OH^-\cdot H_2O\cdot Ar_n$ ions were generated by careful control of an ionized expansion of water vapor seeded directly in the argon carrier gas as described previously.[39] Infrared excitation over the range 600−4500 cm^{-1} was carried out with a LaserVision KTP/KTA OPO/OPA parametric converter pumped by a 10 Hz Nd:YAG laser. The region below 2000 cm^{-1} was generated by mixing in $AgGaSe_2$. This beam was directed into the laser interaction region with a 1 m spherical mirror through a KBr window into the vacuum chamber. The laser path outside the interaction chamber was carefully purged with dry N_2 to ensure minimal variation of laser power due to absorption by ambient water vapor. The reported spectra are the summation of 25−30 individual scans and are normalized to the laser output energy at each wavelength.

3. Theory

Before describing the theory for obtaining spectra from Diffusion Monte Carlo (DMC) wave functions, it is useful to recall that the form of the wave function that is generated by DMC is a Monte Carlo sampling of the ground-state wave function. With the descendent weighting approach,[22] we can also evaluate the value of the wave function, $\psi^{(n)}$, at each of the Monte Carlo points, $q^{(n)}$, and, taken together, the expectation value of a multiplicative operator, O, over the ground-state wave functions is given by[40]

$$\langle O\rangle_0 = \sum_n O(q^{(n)})\psi^{(n)} \tag{1}$$

where the summation is over the Monte Carlo sampling points. Further details of our implementation of DMC for this study are provided elsewhere.[23,31]

As we are calculating the spectrum using only information from the ground-state wave function, there are two sets of issues that need to be considered. One is the choice of vibrational coordinates. While we know that there are $3N - 6$ vibrational coordinates, they are not uniquely defined, and the quality of the results of approximate treatments will depend on the choice of coordinates.[41,42] The second and more central issue involves finding a way to construct all of the quantities that are needed in terms of expectation values of multiplicative operators. The reason for this constraint on the methodology is the desire to generate a straightforward procedure for generating vibrational spectra using ground-state probability amplitudes generated from Diffusion Monte Carlo simulations.

We start by considering the second set of issues and will do this in the context of a one-dimensional oscillator, described as a Morse oscillator. The quantities that we need to evaluate to obtain a spectrum are as follows.

- The first is expressions for excited-state wave functions in terms of ground-state wave functions:

$$\psi_n(q) = f_n(q)\psi_0(q) \tag{2}$$

TABLE 1: Comparison of Approximate and Exact Wave Functions and Energies for a Morse Oscillator

	$v = 1$			$v = 2$		
anharmonicity/ω	overlap	E_1/ω	error/ω	overlap	E_2/ω	error/ω
0.00000	1.00000	1.000	0.00000	1.00000	2.000	0.00000
0.00100	0.99975	0.998	<0.00000	0.99749	1.994	−0.00150
0.00200	0.99950	0.996	<0.00000	0.99498	1.988	−0.00301
0.00400	0.99899	0.992	−0.00001	0.98990	1.976	−0.00603
0.00800	0.99795	0.984	−0.00004	0.97960	1.952	−0.01211
0.01600	0.99580	0.968	−0.00015	0.95835	1.904	−0.02443
0.03200	0.99117	0.936	−0.00061	0.91308	1.808	−0.04975
0.06400	0.98031	0.872	−0.00253	0.80945	1.616	−0.10323
0.12800	0.94926	0.744	−0.01070	0.52713	1.232	−0.22267

- The second is approaches for calculating $\langle\psi_n|H|\psi_n\rangle$ and $\langle\psi_n|\vec{\mu}|\psi_0\rangle$. If we have an approximation for $\psi_n(q)$, in the form of eq 2, the matrix elements of $\vec{\mu}$ and the contribution of the potential energy to the Hamiltonian can be reexpressed as averages over the ground-state probability amplitude.

$$\langle V\rangle_n \approx \frac{\langle f_n^2 V\rangle_0}{\langle f_n^2\rangle_0} \tag{3}$$

and

$$\langle\psi_n|\vec{\mu}|\psi_0\rangle \approx \frac{\langle f_n\vec{\mu}\rangle_0}{\sqrt{\langle f_n^2\rangle_0}} \tag{4}$$

where ψ_0 has been assumed to be normalized. As $\hat{T}$ is not a multiplicative operator, its expectation value will be more challenging to evaluate.

In developing these approaches, we draw from the fact that, in many cases, the harmonic oscillator provides a good zero-order description of molecular vibrations. The functional form of the harmonic oscillator wave functions is given by

$$\varphi_n(q) \propto H_n(\sqrt{\alpha}q)\psi_0(q) \tag{5}$$

where $H_n(x)$ is the nth Hermite polynomial, q represents the displacement of an internal coordinate from its equilibrium value, and

$$\psi_0(q) \propto \exp\left(-\frac{\alpha q^2}{2}\right) \tag{6}$$

This is exactly the functional form in eq 2. Therefore, to approximate $\psi_1(q)$ and $\psi_2(q)$, we use the definitions of $H_1(q) = 2(\alpha q)^{1/2}$ and $H_2(q) = 4\alpha q^2 - 2$, and let

$$\psi_1^{\text{approx}}(q) \propto (q - \langle q\rangle_0)\psi_0(q) \tag{7}$$

$$\psi_2^{\text{approx}}(q) \propto \left[\frac{(q - \langle q\rangle_0)^2}{\langle q^2\rangle_0} - 1\right]\psi_0(q) \tag{8}$$

where α is replaced by $0.5/\langle q^2\rangle_0$, and $\langle O\rangle_0$ represents expectation values taken with respect to the exact ground-state wave function. It should be noted that eqs 7 and 8 are exact for the harmonic oscillators. While in that case $\langle q\rangle_0 = 0$ by symmetry, this will not be true in general.

In Table 1, we report the overlap between $\langle\psi_n^{\text{approx}}|\psi_n\rangle$ for $n = 1$ and 2 for a Morse oscillator over a range of anharmonicities. We find that as long as the anharmonicity is smaller than $\sim 0.016\omega$, the overlap for the $n = 1$ level is larger than 0.995. As a point of comparison, the anharmonicities of the three normal modes in water are 1−2% of the corresponding harmonic frequencies. When $n = 2$, overlaps are smaller than for the $n = 1$ case, but the approximation remains reasonably good. The deterioration with increasing quanta is not surprising due to the fact that the wave functions will be sampling more anharmonic regions of the potential surface.

With this approximation in hand, we can evaluate expectation values of multiplicative operators, such as $V(q)$ as well as matrix elements of the dipole moment operator. Expectation values of operators that involve differentiation of ψ_0 are not as straightforward, as DMC provides a Monte Carlo sampling of the ground-state wave function. To circumvent this problem, we turn, again, to the harmonic oscillator, for which

$$\langle p^2\rangle_n = \hbar m\omega\left(n + \frac{1}{2}\right) = \hbar^2\alpha\left(n + \frac{1}{2}\right) \tag{9}$$

Based on this,

$$\langle T\rangle_n - \langle T\rangle_0 \approx \frac{\hbar^2 n\alpha}{2m} \tag{10}$$

Drawing from the results for the ground state of the harmonic oscillator, for which

$$\alpha \approx \frac{\langle q^2\rangle_0}{\langle q^4\rangle_0 - \langle q^2\rangle_0^2} \tag{11}$$

we calculate the expectation value of the kinetic energy by using the relationship in eq 11 to evaluate α from averages of q^2 and q^4 over the probability amplitude obtained from the anharmonic ground state.

Combining the above expressions, we evaluate the energy of the states of a Morse oscillator with $n = 1$ and 2, using the above approximations for $\psi_1(q)$ and $\psi_2(q)$. The results are reported in Table 1. For anharmonicities that are less than 2% of the frequency, the error in the energy is on the order of 1 part in 10 000. The error for the $n = 2$ energy is roughly a factor of 300 larger. On the other hand, if one compares states for which the overlap of the approximate and the exact wave functions is comparable, the relative error in the energy of the

$n = 2$ level is smaller. On the basis of the above, we expect that this treatment will provide a reasonable approximation to the wave function and energies of the levels with one quantum in a given mode, so long as the anharmonicity is not much larger than 2% of the corresponding frequency.

At this stage, one might ask about using the Virial Theorem to evaluate $\langle T \rangle$ as

$$\langle T \rangle = \frac{1}{2}\langle \vec{r} \cdot \nabla V \rangle \tag{12}$$

This is an obvious alternative solution. Like the approach described above, it allows one to equate the expectation value of the kinetic energy to the expectation value of a multiplicative operator. We investigated this approach and found that it was less accurate than the one described above. We believe this reflects the fact that the Virial Theorem is derived from the fact that ψ is an eigenstate of $\hat{H}$, which is clearly not the case for our ψ_n^{approx}.

While we have shown that we can obtain a reasonable approximation to the wave functions and energies for a one-dimensional system, extensions to multidimensional systems introduce the added complication that the $3N - 6$ internal coordinates are not uniquely defined. Again, we turn to the harmonic oscillator model. For a harmonic ground-state wave function, expressed in normal coordinates, the matrix **S**,

$$S_{i,j} = \langle \psi_0 | (q_i - \langle q_i \rangle_0)(q_j - \langle q_j \rangle_0) | \psi_0 \rangle \tag{13}$$

is diagonal. This is a consequence of the ground-state wave function being expressed as a product of $3N - 6$ gaussians, each of which is a function of one of the normal mode coordinates. We use this result to develop a generalized set of coordinates. Specifically, we evaluate the elements of **S** in terms of expectation values of the displacements of the valence coordinates used to define the geometry of $H_3O_2^-$. We then diagonalize **S** to obtain the transformation between the valence coordinates and the collective coordinates. By using the above definition, we ensure that the linear combinations of displacement coordinates reflect the symmetry of the molecule. This definition also provides a way to obtain a roughly separable set of coordinates that accounts for anharmonicity in the potential, as it is reflected in the ground-state wave function.

To simplify the evaluation of the kinetic energy operator, the coordinates are mass weighted. This is achieved by numerically evaluating the elements of $G^{-1/2}$, where the G is the Wilson G-matrix,[43] the elements of which are given by

$$G_{i,j} = \sum_{\alpha=1}^{3N} \frac{\partial q_i}{\partial x_\alpha} \frac{1}{m_\alpha} \frac{\partial q_j}{\partial x_\alpha} \tag{14}$$

and the elements of the mass-weighted **S**-matrix are evaluated by

$$S_{i,j}^{\text{MW}} = \sum_{k,l} (G^{-1/2})_{i,k} S_{k,l} (G^{-1/2})_{l,j} \tag{15}$$

4. Results and Discussion

4.1. Numerical Details. In this study, we focus on $H_3O_2^-$. The nine internal coordinates are the two terminal OH bond lengths, the OO distance, the two HOO angles, the HOOH torsion angle, and the three Cartesian displacements of the central hydrogen atom from the center of the OO bond. The Cartesian coordinates are in the same axis system as we define our dipole moment operator. Because the values of the matrix elements of the dipole moment operator depend on the embedding of the body-fixed axis system, we employ a modified Eckart embedding.[44] In the case of molecules, like $H_3O_2^-$, which is a nearly symmetric top molecule, it can be hard to develop an algorithm that cleanly defines the direction of the B and C axes after the molecule has undergone large displacements from its equilibrium structure. To account for this, we modified our DMC simulation so as to keep the molecule in a body-fixed axis system. This is achieved by rotating the molecule into an Eckart frame after each displacement. The vibrationally averaged structure of this molecule is a symmetric top. As the reference structure does not reflect this rotational symmetry, we further rotate $H_3O_2^-$ about its A axis so that the B axis lies parallel to the biscector of the HOOH torsion angle. As in our earlier work on this system, we employ the potential and dipole surfaces of Huang, Braams, and Bowman,[14,31] which were evaluated at the CCSD(T)/aug-cc-pvtz level of theory/basis.

TABLE 2: Anharmonic Frequencies of the Nine Fundamentals of $H_3O_2^-$ and $D_3O_2^-$

	$H_3O_2^-$			$D_3O_2^-$		
mode	ViCI[a]	DMC[a]	approx[b]	ViCI[a]	DMC[a]	approx[b]
torsion	132	131	169	108	103	124
OO stretch	515	505	488	493	491	490
wag	576	588	610	398	437	404
rock	465	479	448	319	354	295
z	741	644	763	484	402	504
x	1299	1102	1343	982	792	1008
y	1473		1494	1094		1113
OH-sym	3641	3631	3656	2681	2678	2680
OH-asym	3634	3609	3667	2681	2664	2694

[a] From ref 31. [b] Evaluated using the approximations, described in the text.

4.2. Calculated Energies. In Table 2, we report the energies obtained for the nine fundamentals of $H_3O_2^-$ and $D_3O_2^-$ and compare them to the results of previous studies using the same potential surface.[31] These reflect the results of vibrational−configuration interaction calculations, performed by Huang, Carter, and Bowman, using their MULTIMODE program.[45] The DMC results were obtained by us, employing the fixed-node approximation.[34] Because the earlier study involved calculating each excited state separately, the overall computer time required for that study was more than an order of magnitude greater than in the present study.

Comparing the individual frequencies, one finds differences between all three sets of numbers. On the other hand, the overall agreement is remarkable. Even the very anharmonic z-displacement of the central hydrogen along the OO bond is well-described by the approximations, discussed above. The agreement for the lowest frequency torsion mode is also better than one might expect when one considers the tunneling splitting of roughly 20 cm^{-1} in $H_3O_2^-$. The approximations that were based on a harmonic treatment of molecular vibrations recover the frequency of this mode. The agreement for $D_3O_2^-$ is similar to that for $H_3O_2^-$.

The reported results are based on calculations in which the reference geometry used for embedding the body-fixed axis system is the low-energy saddle point in which the central hydrogen is collinear with the two oxygen atoms and is located at the center of the OO bond. We have also used the planar

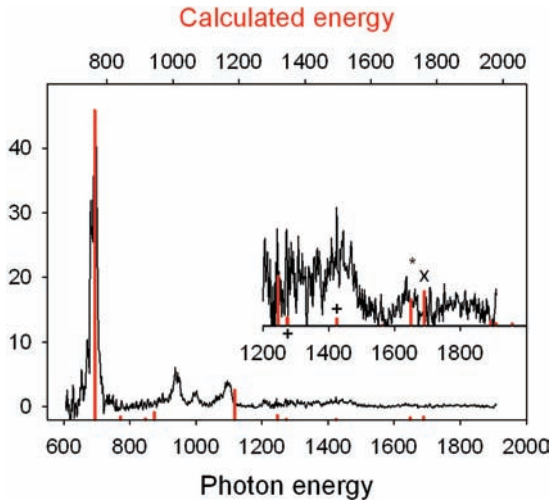

Figure 2. Experimental (black)[1] and calculated (red) spectra for $H_3O_2^-$ between 600 and 2000 cm^{-1}. In the calculated spectrum, the fundamentals in the displacements of the central hydrogen perpendicular to the OO bond are indicated with +'s, while overtones or combination bands involving these modes are shown with *. The overtone in the displacement of the central hydrogen along the OO bond is indicated with an "X". To facilitate comparisons, the calculated spectrum has been shifted by 70 cm^{-1}.

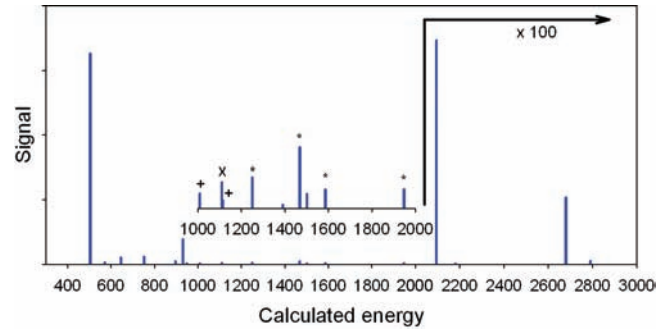

Figure 3. Calculated spectra for $D_3O_2^-$. The fundamentals in the displacements of the central hydrogen perpendicular to the OO bond are indicated with +'s, while overtones or combination bands involving these modes are shown with *. The overtone in the displacement of the central hydrogen along the OO bond is indicated with an "X".

saddle point in which the molecule is in a trans-configuration. The energies shift somewhat due to the fact that the internal coordinates for the central hydrogen atom depend on the choice of embedding, but the overall picture is not affected.

4.3. Calculated Spectrum below 2000 cm^{-1}. While it is reassuring that we can obtain good agreement with previously calculated fundamental frequencies, an important feature of this approach is that it allows us to also evaluate the vibrational spectrum. For these calculations, we only consider transitions originating from the vibrational ground state and calculate the frequencies and intensities of all transitions to states that have at most two quanta of excitation. The calculated spectrum for $H_3O_2^-$ is reported in Figure 2 and overlaid on the recorded argon predissociation spectrum.[1] As the signal in the experimental spectrum has been divided by the power, the signal in the calculated spectrum is given by the magnitude squared of the matrix elements of the dipole moment operator.[3]

In the lower frequency region, the calculated fundamental in the central hydrogen displacement along the OO axis has the largest intensity and a frequency that is roughly 63 cm^{-1} higher than the experimental value. While the difference between the experimental and calculated frequency for this band is larger than we would have liked, this deviation is only slightly larger than the differences obtained when one considers the previously reported calculated frequencies for this mode, reported in Table 2. In fact, if one considers that the harmonic frequency of this mode is close to 1600 cm^{-1},[13,14] it is remarkable that the approximations employed here yield a transition frequency for this mode that is even close to the observed frequency. In addition to computational considerations, based on studies of $H_5O_2^+$, which also contains a symmetrically shared proton, it was found that the frequency of this mode changes by 40 cm^{-1} when the ion is complexed with a neon or argon atom.[20] As such, we are led to expect that the difference between the experimental and calculated frequency reflects, in part, perturbations to the spectrum due to the presence of the argon atom.

If the calculated spectrum is shifted by 70 cm^{-1} so most intense peaks in the two spectra overlap, we find that there are other features that are accounted for in the calculated spectrum. Most notably, there is a calculated peak at 1187 cm^{-1} that agrees well with one of the three features near 1000 cm^{-1} in the experimental spectrum. The origin of this transition in the calculated spectrum is a combination band of the OO stretch and central hydrogen displacement. Interestingly, the frequency of this band in the calculated spectrum is 64 cm^{-1} lower than the sum of the anharmonic frequencies of these two modes. Similar combination bands were assigned in the $H_5O_2^+$ spectrum by Vendrell et al.[9] We do not calculate peaks that correspond to the other two features in this frequency range. We suspect that the additional structure in the experimental spectrum may be due either to combination bands involving three or more quanta of excitation or to perturbations due to the presence of the argon atom. Such perturbations have been seen in other systems.[11,46,47]

An interesting prediction of this study is that overtones and combination bands that involve the displacements of the central hydrogen atom perpendicular to the OO axis are more intense than the fundamentals in this mode. To show these, we have marked the position of the fundamentals in these modes with + and the combination bands with * in Figures 2 and 3. In $H_3O_2^-$, only one such band is below 2000 cm^{-1} and is seen at 1718 cm^{-1}. This transition is in reasonable agreement with a peak in the spectrum and corresponds to a combination band involving one quantum in the rock and one in the displacement of the central hydrogen in the x direction. At nearly the same frequency is the first overtone in the displacement of the central hydrogen along the OO axis, marked with an "X" in the spectrum.

While an experimental spectrum for $D_3O_2^-$ has not been recorded, overall, the spectrum is very similar to that for $H_3O_2^-$. This can be seen by comparing the calculated spectra in Figures 2 and 3.

4.4. $H_3O_2^-$ Spectrum above 2500 cm^{-1}. In Figure 4, we report the spectrum of $H_3O_2^-$ in the range from 2400 to 4500 cm^{-1}. The most intense feature in this region is the sharp peak near 3650 cm^{-1}. This peak has been assigned to the fundamental in the OH stretch.[48] The calculated frequency of this transition is 3667 cm^{-1}, which is in remarkable agreement with experiment.

On the basis of earlier harmonic and anharmonic studies, the broad peaks to the red of the OH stretch fundamental were assigned to overtones or combination bands involving the displacements of the central hydrogen atom[48] and perhaps the torsional mode.[14] In the calculated spectrum, we predict a pair of intense bands at 2574 and 2818 cm^{-1} that correspond to the overtone in one of the modes that corresponds to displacement of the central hydrogen perpendicular to the OO axis and a

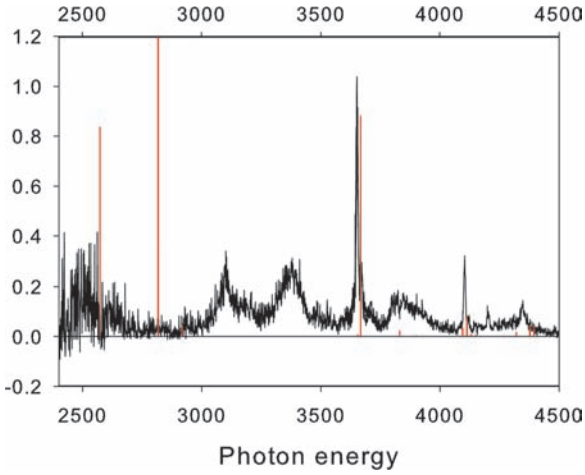

Figure 4. The experimental (black) and calculated (red) spectra for $H_3O_2^-$ between 2400 and 4500 cm^{-1}. The peak in the calculated spectrum at 2818 cm^{-1} is larger than the scale of the plot. It is found to be 2.8 times more intense than the calculated transition at 2574 cm^{-1}.

combination band involving the one quantum of excitation in each of the two coordinates that corresponds to displacement of the central hydrogen atom perpendicular to the OO bond. While the calculated transitions are 500 cm^{-1} lower in frequency than the experimental features, their splitting is consistent with the spacing between the broad bands in the experimental spectrum. In addition, the large intensity, relative to the fundamental in the OH stretch, consistent with the integrated areas of the observed features. Given the differences between the frequencies of these transitions in the experimental and calculated spectra, we are not prepared to make a definitive assignment. We note that while it is unexpected that an overtone would be observed, when the fundamental is not, such an assignment is plausible in the context of the behavior displayed by other anion−water systems. For example, the overtone of the mode corresponding to the displacement of the shared proton perpendicular to the Cl−O axis was found to have about the same intensity as the fundamental in the $Cl^-(H_2O)$ complex. In that case, the fundamental is a perpendicular transition, and the first overtone is a parallel transition.[3,49] This is a case where higher level calculations would be needed to definitively sort out the assignment of these features.

A similarly broad feature is also seen to the blue of the OH stretch fundamental. This band spans from 3890 to 3950 cm^{-1}. The peak in the calculated spectrum at 3831 cm^{-1} is assigned to the combination band involving one quantum of excitation in the asymmetric OH stretch and one quantum of excitation in the torsion mode.

An additional sharper structure to the blue of the OH stretch fundamental is also observed. The two most intense of these correspond well with transitions in the calculated spectrum. Specifically, the peaks near 4150 cm^{-1} correspond to combination bands of the symmetric OH stretch and the rock (4113 cm^{-1}) and the asymmetric OH stretch and the OO stretch (4094 cm^{-1}). Finally, the peaks near 4400 cm^{-1} in the calculated spectrum correspond to combination bands involving the two OH stretches and the displacement of the central hydrogen atom along the OO bond axis.

There is additional less intense structure in the experimental spectrum that is not found in the calculated one. These features likely reflect either higher order combination bands or perturbations to the spectrum due to the argon atom. Despite this, it is remarkable how well such a simple treatment of molecular vibrations captures the spectrum of $H_3O_2^-$, especially given the failure of the harmonic spectrum to reproduce any of the features in the low-frequency region.

5. Summary and Conclusions

In this Article, we have presented an approach for obtaining vibrational spectra using the ground-state Diffusion Monte Carlo wave function. There are several requirements for this approach. First, one needs to have the ability to evaluate the potential and dipole surfaces. This was done by using the fit surfaces of Huang et al.[14,31] In addition, the approach will only be accurate so long as the approximation to the excited-state wave functions is valid. While we have demonstrated the effectiveness of the approach for an anharmonic molecule in which the couplings among the vibrational degrees of freedom are expected to be large, there are cases where the approach will not work. In particular, for the approximation to be valid, the ground-state wave function needs to sample roughly the same regions of configuration space as the excited states of interest. Specifically, in an asymmetric double well system, if the ground state is localized in one well, one will not be able to generate accurate representation of the wave function that is located in the second well using the expression for ψ^{approx} in eq 2. However, the intensity of the transitions between these ground and excited states will be negligibly small. For the case of a symmetric double well system, the results will depend on the range of the coordinate that is sampled, as this will determine the value of $\langle q \rangle_0$ used to evaluate the $\mathbf{S}_{i,j}$. In the case of the torsion in $H_3O_2^-$, the torsion coordinate was only defined in the range from 0 to π, making it into a single minimum problem.

With the above considerations, it appears that the approach outlined above can provide a powerful technique for calculating anharmonic vibrational spectra based only on information about the ground-state probability amplitude. As a demonstration of this, we compare our calculated spectrum for $H_3O_2^-$ to the experimental spectrum for frequencies between 700 and 4500 cm^{-1}. The calculated spectrum shows intensity in the regions where transitions are observed. As importantly, we calculate little or no intensity for transitions in regions of the spectrum where no transitions are observed. This procedure suggests that the activity in the 3000−4000 cm^{-1} range of the spectrum could be due to motions of the bridging proton perpendicular to the OO axis, as opposed to the parallel stretch assignment proposed earlier.[48] One curious aspect of these bands, however, that is not explained by this anharmonic treatment is why these intermediate features are so broad (100 cm^{-1} or so) while other bands are sharp. Identification of the background states accounting for this breadth is therefore one of the key remaining unanswered questions in this surprisingly complex, small system. The possible role of Ar is, of course, always a concern, and it would therefore also be valuable to acquire the spectra of the bare complex or extend the tagging study to include weakly bound Ne or He atoms.

Acknowledgment. A.B.M. and M.A.J. thank the Chemistry Division of the National Science Foundation Division for support of this work. A.B.M. offers special thanks to Professor R. Benny Gerber (Hebrew University) for introducing her to Diffusion Monte Carlo and for numerous discussions over the years. We both acknowledge Benny for his role in shaping the contemporary treatment of molecular vibrations, and for his enthusiastic and effective support of experimental and theoretical efforts by younger colleagues.

References and Notes

(1) Diken, E. G.; Headrick, J. M.; Roscioli, J. R.; Bopp, J. C.; Johnson, M. A.; McCoy, A. B. *J. Phys. Chem. A* **2005**, *109*, 1487–90.

(2) Headrick, J. M.; Diken, E. G.; Walters, R. S.; Hammer, N. I.; Christie, R. A.; Cui, J.; Myshakin, E. M.; Duncan, M. A.; Johnson, M. A.; Jordan, K. D. *Science* **2005**, *308*, 1765069.

(3) Roscioli, J. R.; Diken, E. G.; Johnson, M. A.; Horvath, S.; McCoy, A. B. *J. Phys. Chem. A* **2006**, *110*, 4943–52.

(4) Roscioli, J. R.; McCunn, L. R.; Johnson, M. A. *Science* **2007**, *316*, 249–54.

(5) Asmis, K. R.; Pivonka, N. L.; Santambrogio, G.; Bruemmer, M.; Kaposta, C.; Neumark, D. M.; Woeste, L. *Science* **2003**, *299*, 1375–77.

(6) Fridgen, T. D.; McMahon, T. B.; MacAleese, L.; Lemaire, J.; Maitre, P. *J. Phys. Chem. A* **2004**, *108*, 9008–10.

(7) Asvany, O.; Kumar, P.; Redlich, B.; Hegeman, I.; Schlemmer, S.; Marx, D. *Science* **2005**, *309*, 1219.

(8) Asmis, K. R.; Yang, Y.; Santambrogio, G.; Bruemmer, M.; Roscioli, J. R.; McCunn, L. R.; Johnson, M. A.; Kühn, O. *Angew. Chem., Int. Ed.* **2007**, *46*, 8691–94.

(9) Vendrell, O.; Gatti, F.; Lauvergnat, D.; Meyer, H.-D. *J. Chem. Phys.* **2007**, *127*, 184302/1–17.

(10) Walter, R. A.; Pillai, E. D.; Duncan, M. A. *J. Am. Chem. Soc.* **2005**, *127*, 16599–16610.

(11) Carnegie, P. D.; McCoy, A. B.; Duncan, M. A. *J. Phys. Chem. A*, submitted.

(12) Zhang, X.; Nimlos, M. R.; Ellison, G. B.; Varner, M. E.; Stanton, J. F. *J. Chem. Phys.* **2006**, *124*, 084305.

(13) Xantheas, S. S. *J. Am. Chem. Soc.* **1995**, *117*, 10373–80.

(14) Huang, X. C.; Braams, B. J.; Carter, S.; Bowman, J. M. *J. Am. Chem. Soc.* **2004**, *126*, 5042–5043.

(15) Vazquez, J.; Stanton, J. F. *Mol. Phys.* **2006**, *104*, 377–88.

(16) Chaban, G. M.; Jung, J. O.; Gerber, R. B. *J. Chem. Phys.* **1999**, *111*, 1823–9.

(17) Kjaergaard, H. G.; Garden, A. L.; Chaban, G. M.; Gerber, R. B.; Matthews, D. A.; Stanton, J. F. *J. Phys. Chem. A* **2008**, *112*, 4324–35.

(18) Frisch, M. J.; Trucks, G. W.; Schlegel, H. B.; Scuseria, G. E.; Robb, M. A.; Cheeseman, J. R.; Montgomery, J. A., Jr.; Vreven, T.; Kudin, K. N.; Burant, J. C.; Millam, J. M.; Iyengar, S. S.; Tomasi, J.; Barone, V.; Mennucci, B.; Cossi, M.; Scalmani, G.; Rega, N.; Petersson, G. A.; Nakatsuji, H.; Hada, M.; Ehara, M.; Toyota, K.; Fukuda, R.; Hasegawa, J.; Ishida, M.; Nakajima, T.; Honda, Y.; Kitao, O.; Nakai, H.; Klene, M.; Li, X.; Knox, J. E.; Hratchian, H. P.; Cross, J. B.; Bakken, V.; Adamo, C.; Jaramillo, J.; Gomperts, R.; Stratmann, R. E.; Yazyev, O.; Austin, A. J.; Cammi, R.; Pomelli, C.; Ochterski, J. W.; Ayala, P. Y.; Morokuma, K.; Voth, G. A.; Salvador, P.; Dannenberg, J. J.; Zakrzewski, V. G.; Dapprich, S.; Daniels, A. D.; Strain, M. C.; Farkas, O.; Malick, D. K.; Rabuck, A. D.; Raghavachari, K.; Foresman, J. B.; Ortiz, J. V.; Cui, Q.; Baboul, A. G.; Clifford, S.; Cioslowski, J.; Stefanov, B. B.; Liu, G.; Liashenko, A.; Piskorz, P.; Komaromi, I.; Martin, R. L.; Fox, D. J.; Keith, T.; Al-Laham, M. A.; Peng, C. Y.; Nanayakkara, A.; Challacombe, M.; Gill, P. M. W.; Johnson, B.; Chen, W.; Wong, M. W.; Gonzalez, C.; Pople, J. A. *Gaussian 03*, revision C.02; Gaussian, Inc.: Wallingford, CT, 2003.

(19) Schmidt, M. W.; Baldridge, K. K.; Boatz, J. A.; Elbert, S. T.; Gordon, M. S.; Jensen, J. H.; Koseki, S.; Matsunaga, N.; Nguyen, K. A.; Su, S.; Windus, T. L.; Dupuis, M.; Montgomery, J. A. *J. Comput. Chem.* **1993**, *14*, 1347–63.

(20) Hammer, N. I.; Diken, E. G.; Roscioli, J. R.; Myshakin, E. M.; Jordan, K. D.; McCoy, A. B.; Huang, X.; Carter, S.; Bowman, J. M.; Johnson, M. A. *J. Chem. Phys.* **2005**, *123*, 044308.

(21) Anderson, J. B. *J. Chem. Phys.* **1975**, *63*, 1499–1503.

(22) Suhm, M. A.; Watts, R. O. *Phys. Rep.* **1991**, *204*, 293–329.

(23) McCoy, A. B. *Int. Rev. Phys. Chem.* **2006**, *25*, 77–108.

(24) Quack, M.; Suhm, M. A. *Chem. Phys. Lett.* **1995**, *234*, 71–6.

(25) McCoy, A. B.; Hurwitz, Y.; Gerber, R. B. *J. Phys. Chem.* **1993**, *97*, 12516–22.

(26) Severson, M. W.; Buch, V. *J. Chem. Phys.* **1999**, *111*, 10866–75.

(27) Gregory, J. K.; Clary, D. C. *J. Chem. Phys.* **102**, 7817–29.

(28) Cho, H. M.; Singer, S. J. *J. Phys. Chem. A* **2004**, *108*, 8691–8702.

(29) Brown, A.; McCoy, A. B.; Braams, B. J.; Jin, Z.; Bowman, J. M. *J. Chem. Phys.* **2004**, *121*, 4105–4116.

(30) Thompson, K. C.; Crittenden, D. L.; Jordan, M. J. T. *J. Am. Chem. Soc.* **2005**, *127*, 4954–58.

(31) McCoy, A. B.; Huang, X.; Carter, S.; Bowman, J. M. *J. Chem. Phys.* **2005**, *123*, 064317.

(32) Ceperley, D. M.; Bernu, B. *J. Chem. Phys.* **1988**, *89*, 6316–6328.

(33) Blume, D.; Lewerenz, M.; Whaley, K. B. *J. Chem. Phys.* **1997**, *107*, 9067–78.

(34) Anderson, J. B. *J. Chem. Phys.* **1976**, *65*, 4121–27.

(35) Lee, H.-S.; McCoy, A. B. *J. Chem. Phys.* **2001**, *114*, 10278–87.

(36) Coker, D. F.; Miller, R. E.; Watts, R. O. *J. Chem. Phys.* **1985**, *82*, 3554.

(37) Coker, D. F.; Watts, R. O. *J. Phys. Chem.* **1987**, *91*, 2513–18.

(38) Johnson, M. A.; Lineberger, W. C. In *Techniques for the Study of Ion-Molecule Reactions*; Farrar, J. J. M., Saunders, W. H., Eds.; Wiley: New York, 1988; Vol. XX, p 591.

(39) Robertson, W. H.; Diken, E. G.; Price, E. A.; Shin, J. W.; Johnson, M. A. *Science* **2003**, *299*, 1367–1372.

(40) Auer, B. M.; McCoy, A. B. *J. Phys. Chem. A* **2003**, *107*, 4–12.

(41) Horn, T. R.; Gerber, R. B.; Ratner, M. A. *J. Chem. Phys.* **1989**, *91*, 1813–23.

(42) Mayrhofer, R.; Sibert, E. L. *Theor. Chim. Acta* **1995**, *92*, 107–22.

(43) Wilson, E. B.; Decius, J. C.; Cross, P. C. *Molecular Vibrations*; Dover: New York, 1955.

(44) Louck, J. D.; Galbraith, H. W. *Rev. Mod. Phys.* **1976**, *48*, 69–106.

(45) Bowman, J. M.; Carter, S.; Huang, X. *Int. Rev. Phys. Chem.* **2003**, *22*, 533–549.

(46) McCunn, L. R.; Roscioli, J. R.; Elliott, B. M.; Johnson, M. A.; McCoy, A. B. *J. Phys. Chem. A* **2008**, *112*, 6074–6078.

(47) Ayotte, P.; Kelley, J. A.; Nielsen, S. B.; Johnson, M. A. *Chem. Phys. Lett.* **2000**, *316*, 455–459.

(48) Price, E. A.; Robertson, W. H.; Diken, E. G.; Weddle, G. H.; Johnson, M. A. *Chem. Phys. Lett.* **2002**, *366*, 412–416.

(49) Diken, E. G.; Headrick, J. M.; Roscioli, J. R.; Bopp, J. C.; Johnson, M. A.; McCoy, A. B.; Huang, X.; Carter, S.; Bowman, J. M. *J. Phys. Chem. A* **2005**, *109*, 171–5.

JP811352C